PHYSICAL REVIEW B VOLUME 32, NUMBER 6 15 SEPTEMBER 1985

Theoretical study of subband levels in semiconductor heterostructures

W. Pötz, W. Porod, and D. K. Ferry
Center for Solid State Electronics Research, Arizona State University, Tempe, Arizona 85287
(Received 5 March 1985)

We present an envelope-function approach designed to describe a large class of weakly inhomogeneous semiconductors. This model is a generalization of Kane's eight-band $\mathbf{k}\cdot\mathbf{p}$ model with remote-band effects included in second-order perturbation theory. It is used to study subband levels of single and multiple quantum wells fabricated by layers of GaAs and $Ga_{1-x}Al_xAs$. The dependence of these levels on variations of input parameters such as effective masses and band offsets, as well as sample parameters such as alloy concentration and layer thickness, is investigated. Comparison of our results with experimental data on single $GaAs/Ga_{1-x}Al_xAs$ quantum wells demonstrates that experimental uncertainties in sample length and alloy concentration do not allow a unique determination of the band offsets. For recent data on quasiparabolic wells, we find that the level splittings for electrons and holes cannot always be explained by a unique choice for the offsets. However, in agreement with previous observations, we find that these structures favor nearly symmetric band offsets.

I. INTRODUCTION

Over the last several years, layered structures of semiconductors have become of considerable interest, mostly because they open the door to new semiconductor devices.[1] The fabrication of artificially periodic structures leads to band structures that differ considerably from that of a typical semiconductor. Using thin layers of proper semiconductor alloys allows one to model space-dependent band gaps which may vary over a wide range of energies.[1,2] Sophisticated structures, combined with selective doping of certain layers, have been successfully used to create devices with extremely high carrier mobilities.[3,4] Layered structures have also been used to build elementary devices on the submicrometer scale.[5] On the other hand, such structures are also interesting from a more academic point of view. They allow the study of confinement in microscopic structures, quantization normal to the interfaces, many-particle effects in quasi-two-dimensional systems, and others.[6] Charge carriers in superlattices may show negative differential mobilities and hope exists that they will allow a test of the existence of Bloch oscillations.[7] The properties of layered structures is significantly influenced by how the energy bands of the different materials line up at the interface. Various theoretical approaches have been used to address this question. Envelope-function approaches (EFA's) may be used for moderately thin layer thicknesses. They require the band offsets as input. Attempts to extract the valence- and conduction-band offsets have been made by comparing calculated levels to photoluminescence data on single and multiple quantum wells.[8–13] Other models, such as tight-binding and pseudopotential models, have been used to investigate structures with small layer thicknesses.[14,15] These approaches can, in principle, directly predict the band offsets for (ideal) interfaces. However, despite the considerable effort made over the last few years, this question has not even been solved satisfactorily for the most investigated heterostructures consisting of layers of GaAs and $Ga_{1-x}Al_xAs$.

Here, we present an envelope-function formalism, which is suited to the investigation of layered structures in semiconductors. We use eight Γ-point Bloch functions to expand the wave functions of the confined states and include remote bands in second-order perturbation theory.[16] The basis is chosen such that the spin-orbit interaction is diagonal for $\mathbf{k}=\mathbf{0}$.[17] The eigenvalue problem becomes a system of coupled differential equations in the envelope functions. This system can be decoupled for the individual bands only if motion normal to the interfaces (in the z direction) is studied and terms higher than second order in d/dz are neglected. This model is used to investigate single and multiple quantum wells consisting of thin slabs of GaAs and $Ga_{1-x}Al_xAs$. We calculate the subband levels for single quantum wells of varying thickness and alloy concentration and compare them to experiment. The influence of input parameters (effective masses and band offsets), sensitivity to uncertainties in the sample specification (layer thickness and alloy concentration), as well as deviations from an ideal rectangular barrier profile at the interface are examined. We also study quasiparabolic quantum wells produced by layers of GaAs and $Ga_{1-x}Al_xAs$ of varying layer thickness recently presented by Miller *et al.*[10] In Sec. II we outline the envelope-function model used here. Sections III and IV contain our results and a comparison to experiment for single and multiple quantum wells, respectively. Our summary and conclusions can be found in Sec. V.

II. ENVELOPE-FUNCTION MODEL

The envelope-function approach used here can be viewed as a generalization of Kane's $\mathbf{k}\cdot\mathbf{p}$ method used for bulk materials to describe semiconductors inhomogeneous in space.[16] A set of "near bands" must be selected to serve as a basic upon which to expand the wave function

 ©1985 The American Physical Society

of the system. As we are interested in energy levels close to the main gap of the semiconductor, we use six valence-band states (including spin) from the Γ point (heavy-hole, light-hole, and spit-off band) and two from the conduction-band edge. Then the wave function can be written as

$$\Psi(x,y,z)=\exp(ik_y y)\sum_{j=1}^{8} f_j(z)u_j(x,y,z) , \tag{1}$$

where z denotes the direction normal to the interface and y is a direction parallel to it. In this ansatz it is implicitly assumed that the periodicity of the crystal parallel to the interface is maintained. The basis $\{u_j\}$ is chosen such that the spin-orbit interaction is diagonal at the Γ point and the 8×8 matrix decouples into two 4×4 matrices. This can be accomplished by the following choice for $\{u_j\}$:

$$u_1=S\uparrow,\quad u_2=(\tfrac{2}{3})^{1/2}Z\uparrow+(\tfrac{1}{6})^{1/2}(iY\uparrow+X\downarrow),\quad u_3=-(\tfrac{1}{2})^{1/2}(-iY\uparrow+X\downarrow),\quad u_4=(\tfrac{1}{3})^{1/2}(Z\uparrow-iY\uparrow-X\downarrow) ,$$

$$u_5=-S_\downarrow,\quad u_6=-(\tfrac{2}{3})^{1/2}Z\downarrow+(\tfrac{1}{6})^{1/2}(iY\downarrow+X\uparrow),\quad u_7=-(\tfrac{1}{2})^{1/2}(-iY\downarrow+X\uparrow),\quad u_8=-(\tfrac{1}{3})^{1/2}(Z\downarrow+iY\downarrow+X\uparrow) . \tag{2}$$

X, Y, Z, and S denote the bulk Bloch functions at the valence- and conduction-band edges, and ↑ and ↓ denote the spin direction. With this choice for $\{u_j\}$, one obtains a set of coupled differential equations in the envelope functions $f_j(z)$ with two matrix operators of the form

$$\begin{bmatrix} V(z)+E_c+\alpha k^2-E & P\left[\frac{\partial}{\partial z}\mp\frac{k_y}{2}\right] & \mp\frac{3^{1/2}}{2}Pk_y & \frac{1}{2^{1/2}}P\left[\frac{\partial}{\partial z}\pm k_y\right] \\ -P\left[\frac{\partial}{\partial z}\pm\frac{k_y}{2}\right] & V(z)+\alpha k^2-E & 0 & 0 \\ \mp\frac{3^{1/2}}{2}Pk_y & 0 & V(z)+\alpha k^2-E & 0 \\ \frac{1}{2^{1/2}}P\left[-\frac{\partial}{\partial z}\pm k_y\right] & 0 & 0 & \Delta_0+V(z)+\alpha k^2-E \end{bmatrix} . \tag{3}$$

The upper sign is for the matrix coupling of the first four envelope functions, while the lower sign is for the last four envelope functions, P is $(\frac{2}{3})^{1/2}\hbar/(im_0)$ times the momentum matrix element,[17] and Δ_0 is the spin-orbit splitting at the Γ point. All energies are measured relative to the valence-band edge. $V(z)$ may be an external potential, an image potential, a Hartree term, etc. Furthermore, we use

$$\alpha=\frac{\hbar^2}{2m_0} \tag{4}$$

and

$$k^2=\left[k_y^2-\frac{\partial^2}{\partial z^2}\right] , \tag{5}$$

where m_0 is the free-electron mass.

As we are not interested in motion parallel to the interfaces, we set $k_y=0$. This allows the inclusion of remote-band effects in second-order perturbation theory without introducing coupling terms between the two 4×4 blocks. In addition, the two blocks become identical and the differential equations for $f_3(z)$ $[f_7(z)]$ can be decoupled from the rest of the system. One obtains

$$\left[V(z)+E_c-E-\alpha_c\frac{d^2}{dz^2}\right]f_1(z)+P\frac{d}{dz}f_2(z)+\frac{1}{2^{1/2}}P\frac{d}{dz}f_4(z)=0 , \tag{6a}$$

$$-P\frac{d}{dz}f_1(z)+\left[V(z)-E-\alpha_l\frac{d^2}{dz^2}\right]f_2(z)+\frac{2^{1/2}}{3}(M-L)\frac{d^2}{dz^2}f_4(z)=0 , \tag{6b}$$

$$-\frac{1}{2^{1/2}}P\frac{d}{dz}f_1(z)+\frac{2^{1/2}}{3}(M-L)\frac{d^2}{dz^2}f_2(z)+\left[\Delta_0+V(z)-E-\alpha_{so}\frac{d^2}{dz^2}\right]f_4(z)=0 , \tag{6c}$$

$$\left[V(z)-E-\alpha_h\frac{d^2}{dz^2}\right]f_3(z)=0 , \tag{6d}$$

with

$$\alpha_c = \alpha + A \ , \tag{7}$$

$$\alpha_h = \alpha + M \ , \tag{8}$$

$$\alpha_l = \alpha + \tfrac{1}{3}(2L + M) \ , \tag{9}$$

$$\alpha_{so} = \alpha + \tfrac{1}{3}(L + 2M) \ . \tag{10}$$

A, L, and M are $\mathbf{k}\cdot\mathbf{p}$ coupling terms from the "remote" bands, which in the case of $\mathbf{k}\cdot\mathbf{p}$ calculations are necessary to give the correct effective masses at the Γ point,[16] and $\partial/\partial z$ is replaced by d/dz.

In order to be able to describe inhomogeneous semiconductors, such as alloys with varying concentrations of the constituent atoms or layered structures, one makes the coupling terms P,A,L,M, and the band edges z dependent. This is an intuitive step based on the idea that if the inhomogeneities are weak on the scale of a lattice constant, the carriers locally will still be under the influence of a periodic crystal. However, if they travel on a macroscopic scale, i.e., over many unit cells, the character of the crystal will gradually change. This is expressed in the z dependence of the crystal properties, where z has the character of a macroscopic variable. Therefore, the set of differential equations becomes

$$\left[V(z) + E_c(z) - E - \frac{d}{dz}\alpha_c(z)\frac{d}{dz} \right] f_1(z) + \Pi f_2(z) + \frac{1}{2^{1/2}}\Pi f_4(z) = 0 \ , \tag{11a}$$

$$-\Pi f_1(z) + \left[V(z) + E_v(z) - E - \frac{d}{dz}\alpha_l(z)\frac{d}{dz} \right] f_2(z) + \frac{2^{1/2}}{3}\frac{d}{dz}[M(z) - L(z)]\frac{d}{dz} f_4(z) = 0 \ , \tag{11b}$$

$$-\frac{1}{2^{1/2}}\Pi f_1(z) + \frac{2^{1/2}}{3}\frac{d}{dz}[M(z) - L(z)]\frac{d}{dz} f_2(z) + \left[\Delta_0(z) + V(z) + E_v(z) - E - \frac{d}{dz}\alpha_{so}(z)\frac{d}{dz} \right] \times f_4(z) = 0 \ , \tag{11c}$$

$$\left[V(z) + E_v(z) - E - \frac{d}{dz}\alpha_h(z)\frac{d}{dz} \right] f_3(z) = 0 \ . \tag{11d}$$

$E_v(z)$ is the z-dependent valence-band edge. The matrix has been written in a symmetric form in order to keep it Hermitian. It should be noted that there is no unique way of symmetrizing this matrix, as quantum mechanics does not give a unique prescription of how to convert functions into Hermitian operators. In fact, different symmetrization rules have been used in the literature for phenomenological equations that contain space-dependent effective masses.[18–20] Here, the kinetic-energy terms have been chosen in a BenDaniel-Duke form.[18] In the off-diagonal terms, we chose a symmetric form by using

$$\Pi = \frac{1}{2}\left[P(z)\frac{d}{dz} + \frac{d}{dz}P(z) \right] , \tag{12}$$

where, as in (11), d/dz operates on all z-dependent functions to its right. This set of equations contains both remote-band effects and the k-independent spin-orbit interaction in order to ensure an accurate representation of the bulk properties close to the band edges. $V(z)$ can be used to solve Eqs. (11) self-consistently and to take many-body corrections into account. However, these effects as well as strain at the interface are not investigated here.

The set of coupled differential equations for the envelope functions $f_j(z)$ can be decoupled if terms higher than second order in d/dz are neglected. Then the subband levels associated with band j can be found by solving an eigenvalue equation, which is nonlinear in the eigenvalues E,

$$\left[V(z) + E_j(z) - E - \frac{d}{dz}\alpha_j(z)\frac{d}{dz} - \Pi\beta_j(z)\Pi \right] f_j(z) = 0 \ , \tag{13}$$

where j stands for conduction (c), heavy-hole (h), light-hole (l), or split-off band (so), respectively. $E_j(z)$ is the z-dependent band edge of band j, and

$$\alpha_j(z) = \frac{\hbar^2}{2m_j(z)} \ , \tag{14}$$

where $m_j(z)$ is the free-electron mass, renormalized by remote-band effects, for band j. The $\beta_j(z)$ are given by

$$\beta_c(z) = \frac{1}{E_h(z) - E} + \frac{0.5}{E_{so}(z) - E} \ , \tag{15}$$

$$\beta_h(z) = 0 \ , \tag{16}$$

$$\beta_l(z) = \frac{1}{E_c(z) - E} \ , \tag{17}$$

and

$$\beta_{so}(z) = \frac{0.5}{E_c(z) - E} \ . \tag{18}$$

Equation (13) has to be solved numerically and self-consistently in E. We use a finite-difference method to perform this task. The energy dependence in the $\beta_j(z)$ takes account of (part of the) nonparabolicity in the c, l, and so bands. It should be mentioned that the additional term of second order in d/dz takes the same symmetry structure as the kinetic-energy terms containing $\alpha_j(z)$ when P is independent of z. Equation (13) allows us to study various macroscopically continuous forms of interfaces, as well as semiconductor alloys with continuously varying composition.

Interfaces between two different semiconductors are usually assumed to be macroscopically abrupt. In this case, one has to match the envelope functions of the two different regions at the interface. The discontinuities in the renormalized masses, the momentum matrix element, and the band edges imply that the envelope functions and their first derivatives may be discontinuous. In order to obtain the boundary conditions, we integrate (13) across the interface. Assuming that $f_j(z)$ has only a discontinuity of finite height, one obtains the condition that the expression

$$\{\alpha_j(z)+[P(z)]^2\beta_j(z)\}\frac{d}{dz}f_j(z) \tag{19}$$

has to be continuous across the interface. This means that, at the interface of two different semiconductors, $df_j(z)/dz$ has a step of finite height. Consequently, the second boundary condition is that $f_j(z)$ is continuous across the interface, consistent with the original assumption on its behavior.

The use of the EFA for systems with macroscopically abrupt interfaces may appear doubtful because the effective "potential" varies abruptly at the interface. As this approach is phenomenological, quantitative estimates of the induced errors are difficult. Qualitatively, one can expect it to work well as long as the bulk domains dominate the interface regions, i.e., if the envelope functions are not predominantly localized at the (abrupt) interfaces. For example, this is usually guaranteed if the layer thicknesses are large compared to the lattice constant. Therefore, the solutions obtained have to be checked afterwards for consistency with this assumption. Recently, alternative approaches have been presented and may be used to test the EFA.[14,15]

Here, we want to study layered structures of GaAs and $Ga_{1-x}Al_xAs$. The direct energy gap E_g in $Ga_{1-x}Al_xAs$ is assumed to vary linearly with x. This is a good approximation for $x<0.5$.[21] Then the z-dependent band edges relative to the valence-band edge in GaAs can be written as

$$E_c(z)=E_c(\mathrm{GaAs})+\left[\frac{Q_e}{Q_e+1}\right]\Delta E_g x(z)\ , \tag{20}$$

$$E_h(z)=E_l(z)=-\frac{1}{Q_e+1}\Delta E_g x(z)\ , \tag{21}$$

and

$$E_{so}(z)=\Delta_0(\mathrm{GaAs})+E_h(z)+[\Delta_0(\mathrm{AlAs})-\Delta_0(\mathrm{GaAs})]x(z)\ , \tag{22}$$

where ΔE_g is the increase in E_g per unit x, and Q_e is the band-offset parameter that gives the fraction of ΔE_g that is given to the conduction-band. Here, Q_e is assumed to be independent of x.

The host properties, such as band structures and effective masses of GaAs and AlAs, are fairly well known.[13,22,23] They are needed to determine the coupling parameters P, A, L, and M. The remote-band coupling A is taken from a recent fit to experimental data that included coupling to the Γ_7 and Γ_8 conduction bands.[24] Then P can be determined from the conduction-band mass in GaAs. P is assumed to be the same in GaAs and AlAs. Finally, the remote-band coupling parameters are obtained from the experimentally known h and l masses in GaAs and AlAs. Generally, the alloy $Ga_{1-x}Al_xAs$ is modeled by a linear interpolation of the band structure of GaAs and AlAs. For the main energy gap, bowing is taken into account.[21] The input data taken from experiment are listed in Table I. We need the main energy gap E_g, the position of the Γ_7 conduction band, E_g', the coupling strength between the Γ_6 and $(\Gamma_7+\Gamma_8)$ conduction bands, E_p', the spin-orbit splittings Δ_0 and Δ_0', and effective masses m_i^*. E_p' is assumed equal for GaAs and AlAs. Δ_0' is set equal to zero in AlAs. This leaves Q_e as the only adjustable input parameter once the structure of the sample is defined. Different multiple quantum wells enter via the z-dependent Al concentration $x(z)$.

TABLE I. Bulk parameters used in the envelope-function formalism as defined in the main text and as taken from the literature (Refs. 13, 22, and 24). Energies are in eV, and effective masses are given in free-electron masses m_0.

	GaAs	AlAs
E_g	1.519	3.130
Δ_0	0.341	0.275
$E_g'-E_g$	2.969	1.530
Δ_0'	0.171	0.0
E_p'	5.0	5.0
m_c^*	0.0665	
m_h^*	−0.450	−0.752
m_l^*	−0.088	−0.137

Other simplified versions of $\mathbf{k}\cdot\mathbf{p}$ models have been used to calculate energy levels in semiconductor heterostructure, and a brief comparison of these models to our version may be useful at this point. Independently, Bastard,[20] White and Sham,[25] and Altarelli[26] developed effective-mass models that are similar to each other. Compared to ours, they all neglect the split-off band and confine themselves to abrupt interfaces. In addition, Bastard and White and Sham neglect remote-band effects and set α_c and α_l equal to zero. White and Sham only consider motion normal to the interface. Dawson *et al.*[12] simply applied Bastard's model. Bangert and Landwehr[27] used an effective-mass model for hole states localized at heterojunctions; however, they treated all conduction bands as "remote bands" and considered only abrupt interfaces. To our knowledge, graded interfaces have only been studied by effective-mass equations of the BenDaniel-Duke type,[28] which arise from a one-band effective-mass model with a space-dependent effective mass.

III. SINGLE QUANTUM WELLS

Single quantum wells consisting of a layer of GaAs in between $Ga_{1-x}Al_xAs$ are the simplest and most investigated layered structures to produce quantized levels. Several systematic investigations of these structures have been reported in the literature. Dingle and co-workers[8,9] measured optical interband transition energies and interpreted them in terms of a simple effective-mass model, assuming rectangularly shaped space-dependent band edges across the sample. They extracted a value of 0.85 for the relative conduction-band offset Q_e from their experimental data. This value seems to have been unquestioned for several years. More recently, however, doubts as to the correctness of this value have arisen. This is partly due to transport measurements, most of which indicate a lower value for Q_e.[29–32] However, Wu and Yang[32] did find agreement of their results with $Q_e=0.85$. Also, recent

data obtained from excitation spectroscopy experiments of the photoluminescence for both rectangular and quasiparabolic quantum wells were interpreted with relative conduction-band offsets Q_e of 0.51 and 0.57. However, rather unusual values for the heavy- and light-hole masses were used to fit the data.[10,11] Dawson *et al.*[12] took great care in sample preparation to get an accurate value for the thickness of the GaAs layer. They concluded Q_e to be about 0.75 from fairly narrow single quantum wells. On the other hand, in another recent paper Xu *et al.*[13] could fit their photoluminescence data on multiple quantum wells with the established value of 0.85, provided nonparabolicity in the conduction band of GaAs was taken into account. Also, White and Sham reported a successful fit of optical interband transition energies using a simplified $\mathbf{k}\cdot\mathbf{p}$ model with $Q_e=0.85$.[25]

The band offsets represent very important characteristics of semiconductor interfaces, which need to be known accurately in order to successfully design new devices with space-dependent energy gaps ("band-gap engineering"). Here, we try to find the origin of the large spread in the extracted values for Q_e. First, we calculate the subband levels for the samples presented by Dingle and coworkers[8,9] and Miller *et al.*[11] using the input data from Table I. From the subband energies, we obtain the optical interband transition energies E_{nmi}. Here, n and m label the conduction-band and valence-band associated levels involved in the transition (i specifies the type of hole). If $n=m$, the transition energies are simply denoted by E_{ni}. Excitonic effects can be taken into account by subtracting the exciton binding energies from our calculated transition energies. For Dingle's data, we use his values for the exciton binding energies to account for their contribution in the experimental data.[9] Miller's data were already presented in such a way that the major exciton contributions were eliminated.[11] The agreement of our results with these experimental data is rather disappointing. No value for Q_e between 0.5 and 0.9 can reproduce them in a consistent way. For example, comparison with Dingle's data favors $Q_e=0.85$ for the heavy-hole transition energies conserving the level index (E_{nh}), values around 0.6 for E_{nl}, and smaller than 0.5 for E_{13h}. Unfortunately, these data do not show error bars. Similar problems occur when we try to determine Q_e from Miller's data. For several transition energies the experimental uncertainties from samples that differ only slightly in L_z are larger than the range of energy that can be covered by Q_e between 0.5 and 0.9 (e.g., E_{2h} for $L_z=100$ Å). In other cases, none of these values for Q_e can reproduce the measured transition energy.

In order to find the sources for this disagreement, we systematically vary the input data within their estimated experimental error bars. A typical outcome of such a study is given in Fig. 1, performed for a single quantum well with the nominal values $L_z=100$ Å and $x=0.2$. It shows clearly that uncertainties in the sample length represent the main source for uncertainties in the calculated values for transition energies. Variations in x have a smaller effect; however, it is still of the same order as effects due to variations in Q_e within its discussed limits. Variation of the heavy-hole mass in GaAs from $0.45m_0$ to $0.35m_0$, which was claimed to be required to reproduce experimental data,[11] changed the transition energies only slightly. Replacing the discontinuous potential at the interface by a smooth potential step of width $d\leq 20$ Å was found to have an almost negligible effect, particularly on the lower levels in the well, which is in qualitative agreement with the results of Stern and Schulman.[28]

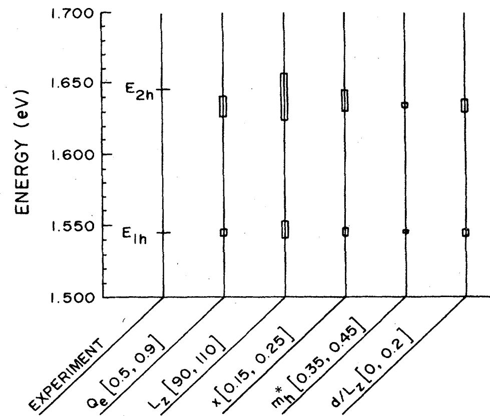

FIG. 1. Transition energies E_{1h} and E_{2h} of a single quantum well as a function of various structure and material parameters. The nominal values for the present sample are $L_z=100$ Å, $x=0.20$, and $Q_e=0.5$ (Ref. 9).

Much better agreement can be found with the data presented by Dawson *et al.*,[12] who realized that small and accurate values for L_z were essential for a successful determination of Q_e. For example, one of their samples was specified by $L_z=71$ Å and $x=0.26$. The measured transition energies, with exciton effects already extracted, were $E_{1h}=1.5807$ eV, $E_{1l}=1.5972$ eV, and $E_{2h}=1.7329$ eV, all within ±0.001 eV. For $Q_e=0.7$, we find agreement for all energies within 3 meV; for $Q_e=0.9$, within 5 meV; and for $Q_e=0.5$, within 24 meV. However, despite the relatively small uncertainties of one monolayer in the sample length, we find that the relative uncertainty in L_z is high enough to allow only a fairly rough estimate of Q_e of about 0.7 ± 0.1. A disadvantage of narrow wells is that only a few subband levels exist. Consequently, only a few optical transitions can be observed, of which few reveal useful sensitivity to the choice of the band offsets. In the present case, for instance, only E_{2h} shows a strong dependence on Q_e.

IV. QUASIPARABOLIC WELL

Very recently the first successful fabrication of layered structures of GaAs and $Ga_{1-x}Al_xAs$ to simulate a parabolic band profile between the confining $Ga_{1-x}Al_xAs$ layers was reported. By varying the layer thicknesses quadratically with the distance from the center of the sample, Miller *et al.*[10] could show that the subband levels associated with valence and conduction bands were spaced nearly equidistantly in energy. From level splittings extracted from three different samples, they concluded a value $Q_e=0.51$ and later 0.57 by use of a one-band EFA.[10,11]

TABLE II. Calculated energy splittings ΔE_i of subband levels associated with quasiparabolic quantum wells for the nominal values for total length L_z and relative Al concentration x compared to experimental results (Ref. 10). All energies are in meV. MQW denotes multiple quantum well.

	$Q_e=0.51$		$Q_e=0.85$		
	MQW	Parabolic	MQW	Parabolic	Experiment
		Sample 1 ($L_z=510$ Å and $x=0.30$)			
ΔE_c	28.8	26.6	35.4	34.4	22.3
ΔE_h	10.2	9.8	5.6	5.4	8.4
ΔE_l	23.6	22.0	13.6	12.2	16.9
ΔE_{so}	16.0	8.0	14.8	7.0	
		Sample 2 ($L_z=325$ Å and $x=0.29$)			
ΔE_c	42.8	41.0	53.2	52.0	40.1
ΔE_h	16.0	15.0	8.8	8.2	15.6
ΔE_l	35.0	33.9	19.8	18.8	27.9
ΔE_{so}	23.6	22.8	12.0	10.8	
		Sample 3 ($L_z=336$ Å and $x=0.30$)			
ΔE_c	43.0	40.4	53.4	52.0	33.1
ΔE_h	15.6	14.7	8.8	8.1	12.4
ΔE_l	35.2	33.4	20.0	18.6	23.7
ΔE_{so}	24.0	22.4	12.0	10.6	

Here, we apply our model to these structures and try to determine if they allow an extraction of the band lineups without any modification of bulk parameters, such as effective masses. First we discuss the results obtained for the three samples using the nominal values for L_z and x. The results for $Q_e=0.51$ and 0.85 are given in Table II. These calculations confirm the parabolic character of the structures. The level splittings for the lowest levels are nearly equidistant. For example, for conduction-band associated states, the splitting typically decreases by 1 meV when going to the next higher level. However, for all samples and for both conduction- and valence-band associated levels we obtain splittings that are consistently higher than those extracted by Miller *et al.*[10] from the exciton spectrum. Their extraction of the energy splittings from excitonic peaks was based on some simplifying assumptions on the exciton binding energies. First, excitons involving heavy holes were assumed to have the same binding energy as those formed with light holes. Calculations show that they differ by typically 1–2 meV for these sample lengths.[33–35] Secondly, the excitonic energies for excited states were assumed equal to those of the ground state. This assumption may not be as good as for single quantum wells because the extent of the wave functions differs more strongly for the levels of a parabolic potential. From inspection of the experimental data given in Ref. 10, and including the difference in excitonic energies for h and l holes, we extract $\Delta E_c=24$ meV, $\Delta E_h=8.5$ meV, and $\Delta E_l=19$ meV from experiment. This improves agreement with theory somewhat. The remaining differences indicate that the nominal values for L_z were too small and/or the alloy parameter x was estimated too large. A change of Q_e can obviously not improve the agreement, as is demonstrated for $Q_e=0.85$ in Table II. It should be mentioned that the numerical errors in the calculated level splittings for layered structures are about 1 meV.

The fact that these multiple quantum wells (some slabs containing less than a monolayer of deposited material) reveal a quasiparabolic energy spectrum demonstrates the insensitivity of the confined states to the microscopic details of the structure. This is exactly the main assumption made in the envelope-function approach. In order to demonstrate this insensitivity within our model, we also perform calculations for truly parabolic profiles. The results are also given in Table II. Considering numerical uncertainties for the layered structures, the results are practically identical. The level splittings obtained are typically 1–2 meV below the values obtained for the corre-

TABLE III. Parametric study for sample 1 with nominal $L_z=510$ Å and $x=0.3$. For comparison, the experimental level splittings were reported as $\Delta E_c=22.3$ meV, $\Delta E_h=8.4$ meV, and $\Delta E_l=16.9$ meV (Ref. 10).

	Q_e			
	0.51	0.60	0.65	0.85
	$L_z=507$ Å and $x=0.25$			
ΔE_c	24.2	26.4	27.6	31.6
ΔE_h	8.9	8.0	7.6	5.2
ΔE_l	20.2	18.2	17.0	11.2
	$L_z=550$ Å and $x=0.25$			
ΔE_c	22.6	24.4	25.4	29.0
ΔE_h	8.2	7.4	6.9	4.5
ΔE_l	18.6	16.8	15.4	10.34
	$L_z=550$ Å and $x=0.30$			
ΔE_c	24.8	26.4	27.8	31.8
ΔE_h	9.0	8.2	7.6	5.0
ΔE_l	20.4	18.4	17.2	11.2

TABLE IV. Parametric study for sample 3 with nominal $L_z=336$ Å and $x=0.3$. The experimental values for the level splittings are $\Delta E_c=33.1$ eV, $\Delta E_h=12.4$ eV, and $\Delta E_l=23.7$ eV (Ref. 10).

	Q_e			
	0.51	0.60	0.65	0.85
	$L_z=336$ Å and $x=0.30$			
ΔE_c	40.4	43.8	45.4	52.0
ΔE_h	14.7	13.2	12.4	8.1
ΔE_l	33.4	30.2	28.2	18.6
ΔE_{so}	22.4	20.0	18.6	10.6
	$L_z=350$ Å and $x=0.30$			
ΔE_c	39.0	42.0	43.7	50.0
ΔE_h	14.1	12.8	11.9	7.8
ΔE_l	32.0	27.8	27.2	17.8
	$L_z=360$ Å and $x=0.25$			
ΔE_c	34.4	37.2	38.8	44.2
ΔE_h	12.5	11.3	10.6	6.9
ΔE_l	28.4	25.7	24.1	15.8

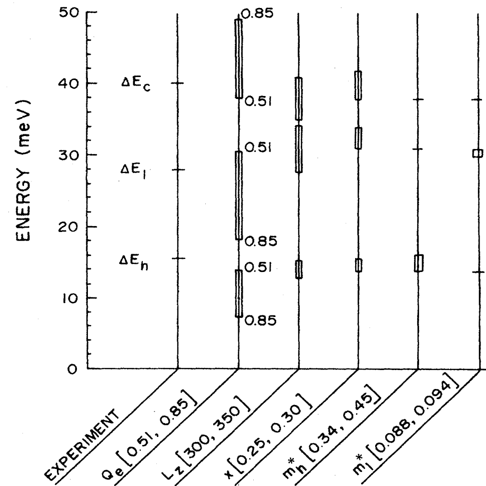

FIG. 2. Dependency of subband level splittings of a parabolic quantum well [sample 2 of Miller *et al.* (Ref. 10)] on various parameters. The nominal values used are $L_z=325$ Å, $x=0.25$, and $Q_e=0.51$. Experimental values are given for comparison.

sponding layered structure, which is almost within the numerical uncertainty.

In order to achieve better agreement with experiment, we vary L_z and x within the experimental error bars using parabolic band profiles. The results for sample 1 are given in Table III and show that increasing the sample length to its upper limit and reducing x towards its lower limit gives good agreement with experiment, if Q_e is chosen to be between 0.5 and 0.65. From this comparison, a value as high as 0.85 can be clearly ruled out. This finding is in agreement with the conclusions drawn by Miller *et al.*[10] However, here no modification in the effective masses from their fairly established bulk values is required. The agreement is somewhat less favorable for the other, shorter samples. To demonstrate this, our results on sample 3 are summarized in Table IV. Following the insight gained from Table II, we increased the sample length to 350 and 360 Å. Again, values for Q_e between 0.5 and 0.65 give fairly good agreement, whereas $Q_e=0.85$ can be ruled out. However, for any value chosen, one or the other level splitting will differ by several meV. Similar conclusions hold for sample 2. We suppose that these slight disagreements can be traced back to somewhat incorrect measurements of the length of samples 2 and 3. Both the values for L_z and x are nearly the same, whereas the measured level splittings differ considerably. Within our model, this cannot be explained by the small changes in L_z. It should be stressed that modified values for hole masses are not sufficient to significantly improve agreement with experiment. They would mainly affect the splitting of hole levels, but could not explain why ΔE_c from theory tends to exceed the experimental value (e.g., 33.1 meV for sample 3). Also, we believe that a value for Q_e extracted by using values for effective masses that differ considerably from the established bulk values is questionable.

Finally, in order to demonstrate the sensitivity of the level splittings on the sample parameters more vividly, results for sample 2 are shown in Fig. 2. Comparison with Fig. 1 shows that now the choice of Q_e has a stronger influence on the level structure than for single quantum wells. Values for Q_e around 0.6 have to be favored against those around 0.8. Different values for m_h^* have only a noticeable influence on ΔE_h.

V. SUMMARY AND CONCLUSIONS

In the first part of this paper, we present a many-band effective-mass model to describe the energy spectrum of semiconductors inhomogeneous in one space dimension. Eight Γ-point wave functions (six from the valence band and two from the conduction band) serve as a basis to expand the wave functions. This leads to a representation of the eigenvalue problem in the form of a system of coupled differential equations in the envelope functions. Remote-band effects are included in second-order perturbation theory. Inhomogeneities in the material are taken into account by space-dependent $\mathbf{k}\cdot\mathbf{p}$ matrix elements, which, by symmetry, also lead to additional gradient terms in the eigenvalue equations. Therefore, this model is general enough to be applicable to a wide class of graded semiconductors.

In the second part, a simplified version of this model is used to calculate the energy levels corresponding to confined states in single and multiple quantum wells, consisting of layers of GaAs and $Ga_{1-x}Al_xAs$. For single quantum wells, we demonstrate that experimental uncertainties in layer thickness and alloy composition make it nearly impossible to extract the band offsets with satisfactory accuracy. Details in the potential profile at the interface, as well as uncertainties in the heavy-hole mass have only a minor effect on the results. In contrast, our studies of multiple quantum wells that simulate parabolic profiles clearly favor a value of Q_e around 0.6, in agreement with

previous conclusions.[10,11] However, no "optimal" value for Q_e could be obtained for these samples and only a rather broad range for the value of Q_e between 0.5 and 0.65 could be extracted. The energy levels of these structures show a significantly increased sensibility to the choice of the offsets relative to single quantum wells. Provided that fabricational uncertainties can be improved, this type of multiple quantum well may finally allow the determination of the accurate value for Q_e. At present, various potential profiles simulated by multilayer structures are under investigation with respect to their sensitivity to the value of Q_e.[36]

ACKNOWLEDGMENTS

The authors would like to thank Dr. A. C. Gossard and Dr. G. Duggan for helpful communication. This work was supported in part by the U.S. Army Research Office, Department of the Army.

[1]F. Capasso, W.-T. Tsang, and G. F. Williams, IEEE Trans. Electron Devices **ED-30**, 381 (1983).

[2]See, e.g., V. Narayanamurti, Physics Today **37**(10), 24 (1984).

[3]E. E. Mendez, P. J. Price, and M. Heiblum, Appl. Phys. Lett. **45**, 294 (1984).

[4]W. I. Wang, E. E. Mendez, and F. Stern, Appl. Phys. Lett. **45**, 639 (1984).

[5]T. C. L. G. Sollner, W. D. Goodhue, P. E. Tannenwald, C. D. Parker, and D. D. Peck, Appl. Phys. Lett. **43**, 588 (1983).

[6]T. Ando, A. B. Fowler, and F. Stern, Rev. Mod. Phys. **54**, 437 (1982).

[7]R. O. Grondin, W. Porod, J. Ho, D. K. Ferry, and G. J. Iafrate, Superlattices Microstruct. **1**, 97 (1985).

[8]R. Dingle, W. Wiegmann, and C. H. Henry, Phys. Rev. Lett. **33**, 827 (1974).

[9]R. Dingle, in *Festkörperprobleme XV*, edited by H. J. Queisser (Pergamon/Vieweg, Braunschweig, 1975), p. 21.

[10]R. C. Miller, A. C. Gossard, D. A. Kleinman, and O. Munteanu, Phys. Rev. B **29**, 3740 (1984).

[11]R. C. Miller, D. A. Kleinman, and A. C. Gossard, Phys. Rev. B **29**, 7085 (1984).

[12]P. Dawson, G. Duggan, H. I. Ralph, K. Woodbridge, and G. W. 't Hooft, Superlattices Microstruct. **1**, 231 (1985).

[13]Z. Y. Xu, V. G. Kreismanis, and C. L. Tang, Appl. Phys. Lett. **43**, 415 (1983).

[14]J. N. Schulman and T. C. McGill, Phys. Rev. Lett. **26**, 1680 (1977).

[15]M. Jaros and K. B. Wong, J. Phys. C **17**, L765 (1984).

[16]E. O. Kane, in *Semiconductors and Semimetals, Physics of III-V Compounds*, edited by R. K. Willardson and A. C. Beer (Academic, New York, 1966), Vol. 1, p. 75.

[17]G. E. Marques and L. J. Sham, Surf. Sci. **113**, 131 (1982).

[18]D. J. BenDaniel and C. B. Duke, Phys. Rev. **152**, 683 (1966).

[19]G. Bastard, J. K. Furdyna, and J. Mycielski, Phys. Rev. B **12**, 4358 (1975).

[20]G. Bastard, Phys. Rev. B **25**, 7584 (1982).

[21]R. Dingle, R. A. Logan, and J. R. Arthur, Jr., in *Gallium Arsenide and Related Compounds (Edinburgh, 1976)*, edited by C. Hilsum (IOP, London, 1977), Vol. 33a, p. 210.

[22]M. Cardona, in *Landolt-Börnstein, Zahlenwerke aus Naturwissenschaft und Technik, Neue Serie* (in German), edited by K. H. Hellwege (Springer, Berlin, 1981), Vol. 17a.

[23]B. A. Vojak, W. D. Laidig, N. Holonyak, Jr., M. D. Camras, J. J. Coleman, and P. D. Dapkus, J. Appl. Phys. **52**, 621 (1981).

[24]L. G. Shantharama, A. R. Adams, C. N. Ahmad, and R. J. Nicholas, J. Phys. C **17**, 4429 (1984).

[25]S. R. White and L. J. Sham, Phys. Rev. Lett. **47**, 879 (1981).

[26]M. Altarelli, Physica **117&118B**, 747 (1983).

[27]E. Bangert and G. Landwehr, Superlattices Microstruct. **1**, 363 (1985).

[28]F. Stern and J. N. Schulman, Superlattices Microstruct. **1**, 303 (1985).

[29]H. Kroemer, W.-Y. Chien, J. S. Harris, Jr., and D. D. Edwall, Appl. Phys. Lett. **36**, 295 (1980).

[30]R. People, K. W. Wecht, K. Alavi, and A. Y. Cho, Appl. Phys. Lett. **43**, 118 (1983).

[31]K. Hirakawa, H. Sasaki, and J. Yoshino, Appl. Phys. Lett. **45**, 253 (1984).

[32]C. M. Wu and E. S. Yang, J. Appl. Phys. **51**, 2261 (1980).

[33]R. C. Miller, D. A. Kleinmann, W. T. Tsang, and A. C. Gossard, Phys. Rev. B **24**, 1134 (1981).

[34]R. L. Greene, K. K. Bajaj, and D. E. Phelps, Phys. Rev. B **29**, 1807 (1984).

[35]C. Priester, G. Allan, and M. Lannoo, Phys. Rev. B **30**, 7302 (1984).

[36]W. Pötz and D. K. Ferry, preceding paper, Phys. Rev. B **32**, 3863 (1985).